

Magnetotransport and interdiffusion characteristics of magnetic tunnel junctions comprising nano-oxide layers upon exposure to postdeposition annealing

In Chang Chu, Min Sung Song, Byong Sun Chun, Seong Rae Lee, Young Keun Kim*

Department of Materials Science and Engineering, Korea University, Anam-Dong, Seongbuk-Gu, Seoul 136-713, South Korea

Received 24 April 2005; accepted 20 May 2005 by H. Akai

Available online 9 June 2005

Abstract

Magnetic tunnel junction (MTJ) structures based on underlayer (CoNbZr)/bufferlayer (CoFe)/antiferromagnet (IrMn)/pinned layer (CoFe)/tunnel barrier (AlO_x)/free layer (CoFe)/capping (CoNbZr) have been prepared to investigate thermal degradation of magnetoresistive responses. Some junctions possess a nano-oxide layer (NOL) inside either in the underlayer or bufferlayer. The main purpose of the NOL inclusion was to control interdiffusion path of Mn from the antiferromagnet so that improved thermal stability could be achieved. The MTJs with NOLs were found to have reduced interfacial roughness, resulting in improved tunneling magnetoresistance (TMR) and reduced interlayer coupling field. We also confirmed that the NOL effectively suppressed the Mn interdiffusion toward the tunnel barrier by dragging Mn atoms toward NOL during annealing. © 2005 Elsevier Ltd. All rights reserved.

PACS: 75.70.Cn; 85.75.Dd

Keywords: A. Nano-oxide layer; D. Interlayer diffusion; D. Magnetic tunnel junction

Magnetic tunnel junctions (MTJs) are currently of considerable interest largely because of their potential application as nonvolatile magnetic memory cells and magnetic field sensors [1]. For these applications the most useful MTJs are exchange-biased structures in which one of the ferromagnetic layers is pinned by exchange bias with an antiferromagnetic layer such as IrMn. In particular, for memory applications, the thermal stability is of critical importance because of high processing temperature. However, the TMR response of MTJs with Mn-based antiferromagnets often reduces significantly upon exposure to elevated temperature due to Mn interdiffusion [2,3] or imperfection in the barrier [4].

In the present study, we have made an attempt to control

the Mn diffusion profile by devising a nano-oxide layer (NOL) structure inside the MTJ. The NOL structure had been implemented first in giant magnetoresistive IrMn spin-valves [5,6] to promote in-plane spin-dependent scattering originating from specularly [7]. Though this effect is not critical for current perpendicular-to-plane devices like MTJs, we could at least achieve relatively better interfacial flatness for the MTJs with NOLs because they would suppress the columnar growth of subsequent layers. Note that it was not our intention to optimize TMR ratio. Instead, an emphasis was given on understanding of NOL effects on magnetotransport and thermal behaviors.

The reference MTJ structure consisting of Si/SiO₂/underlayer Co_{85.5}Nb₈Zr_{6.5}/bufferlayer Co₉₀Fe₁₀ 10/antiferromagnetic Ir₂₀Mn₈₀ 7.5/magnetically pinned layer Co₉₀Fe₁₀ 3/tunnel barrier Al 1.6 + oxidation/magnetically free layer Co₉₀Fe₁₀ 3/capping Co_{85.5}Nb₈Zr_{6.5} 2 (in nm) was prepared by a four-target rf magnetron sputtering system

* Corresponding author. Tel./fax: +81 2 3290 3281.

E-mail address: ykim97@korea.ac.kr (Y.K. Kim).

under typical base pressure below 3×10^{-7} Torr. Deposition was done under Ar pressure of 2 mTorr. A Co target with small Nb and Zr chips added were used to get proper composition of the CoNbZr films. CoNbZr was chosen as an underlayer material because it is amorphous and proven to offer rather flat surface [8]. Tunnel barriers were formed by oxidizing 1.6 nm thick Al layers under rf plasma environment. A magnetic field of 300 Oe was applied to induce uniaxial anisotropy during deposition.

Three sample sets depending on the location of NOL were prepared: (a) a reference structure mentioned above without NOL, (b) an NOL in the middle of CoNbZr underlayer, and (c) an NOL in the middle of CoFe bufferlayer. The NOLs were formed by oxygen plasma oxidation of CoNbZr and CoFe for sample (b) and (c), respectively. The power density for both CoNbZr deposition and CoNbZr-NOL formation was kept at 2.8 W/cm^2 , whereas that for CoFe and CoFe-NOL was 1.1 W/cm^2 . Each NOL was formed under 5 mTorr of pure oxygen environment for 50 s. Note that we did not intend to optimize either the NOL thickness or microstructure.

Junctions were patterned by a set of metal shadow mask with an opening area of $200 \times 200 \mu\text{m}^2$. A series of postdeposition annealing was performed to investigate thermal responses at $150\text{--}350^\circ\text{C}$ for 10 min in 3×10^{-6} Torr vacuum under an applied magnetic field of 500 Oe. Various analytical methods such as atomic force microscopy (AFM), Auger electron spectroscopy (AES), and cross-sectional transmission electron microscopy (XTEM) were employed for interfacial roughness, interlayer diffusion, and microstructure characterizations, respectively.

Fig. 1 displays the cross-sectional micrographs of three MTJ structures annealed at 300°C for 1 h. The CoNbZr underlayers show amorphous structure. Both tunnel barrier and NOLs appearing in Fig. 1(b) and (c) are also amorphous. All three samples have very low interfacial roughness as manifested by the uniform and flat tunnel barrier formation. A thicker NOL in Fig. 1(b) is due to higher oxidation plasma density as mentioned before. To confirm the interfacial roughness changes in detail, we have employed AFM for three samples structures before IrMn deposition. Because the AFM measurement was done ex situ and the roughness values were taken as an average of multiple $1 \times 1 \mu\text{m}^2$ area scans, the measured values may be slightly different compared to the realistic ones. The measured rms roughness values are (a) 0.1 nm for CoNbZr 4/CoFe 10 nm, (b) 0.06 nm for CoNbZr 2/NOL/CoNbZr 2/CoFe 10 nm, and (c) 0.08 nm for CoNbZr 4/CoFe 5/NOL/CoFe 5 nm surfaces. The presence of NOL offered reduction in interfacial roughness, at least, for the bottom portion of the MTJ because amorphous NOL helped to retard the columnar growth of subsequent layers. In particular, for the case of sample (b), it is thought that the presence of a very thin (2 nm) amorphous CoNbZr also contributed to limit the crystal growth of the subsequent CoFe layer.

The magnetotransport properties such as MR ratio,

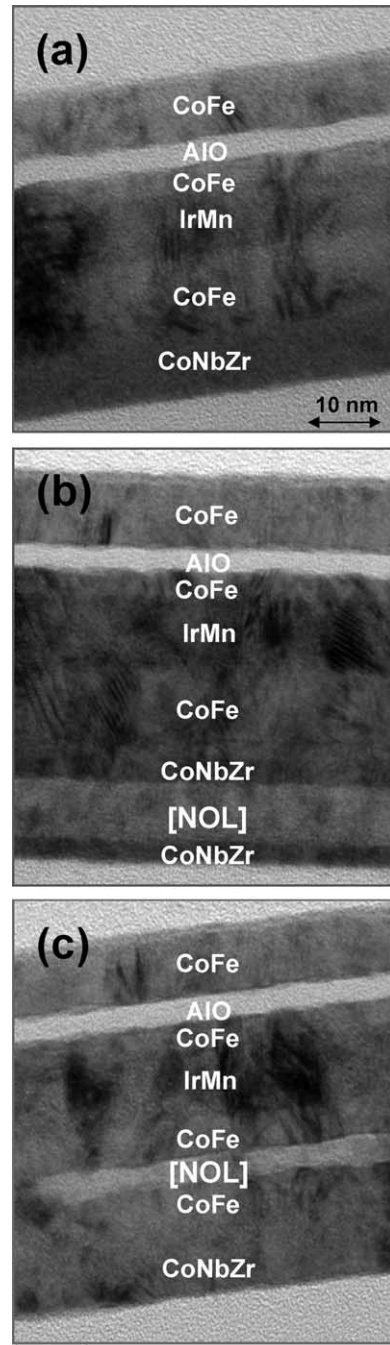


Fig. 1. Cross-sectional TEM micrographs of three MTJ structures annealed at 300°C for 1 h under magnetic field of 500 Oe: (a) without an NOL, (b) an NOL inside bufferlayer, and (c) an NOL inside underlayer.

exchange bias field H_{ex} , and interlayer coupling field H_{in} , of three MTJs as as-deposited state are depicted in Fig. 2. The H_{ex} value indicates the strength of exchange between the IrMn and pinned CoFe layers (larger, the better) defined as a

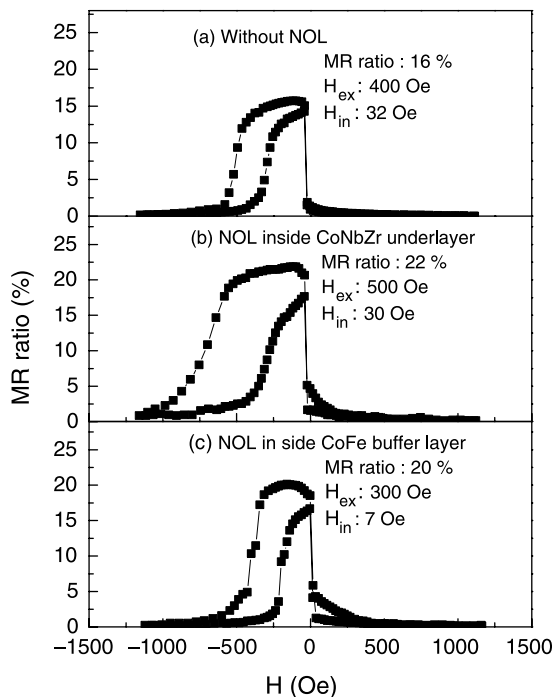


Fig. 2. Magnetoresistive responses of MTJs at as-deposited states.

distance from the zero field to the middle of a major loop (usually a fat one appeared far left from the zero field). Meanwhile, the H_{in} is the strength of coupling between the free and pinned layers through the barrier layer (smaller, the better) defined as a distance from the zero field to the middle of a minor loop (a very thin one located in the vicinity of the zero field). Note that zero H_{in} means there is no shift in the minor loop from the zero field axis. The increase of MR ratios for NOL consisting junctions such as (b) 22% and (c) 20%, compared to the junction (a) 16%, can be attributed to the reduction in interfacial roughness as mentioned previously. The junction resistance was increased from 160 Ω for sample (a), to 400 Ω for sample (b), and to 1700 Ω for sample (c). More uniform and flat tunnel barrier would also result in reduction in interlayer coupling between free and pinned CoFe layers. In fact, this was evidenced in junction (c) where H_{in} was reduced from 32 to 7 Oe compared to the reference junction (a). However no significant reduction in H_{in} was observed for junction (b) though this junction has very flat interface. According to the Kools' interlayer coupling model [9], H_{in} is a function of various parameters including the layer thickness, and interfacial waviness with amplitude h and wavelength λ . The h and λ can be interpreted as the interfacial roughness between the ferromagnetic layer and space layer (e.g. the roughness of the CoFe pinned layer), and the grain size, respectively. Due to the presence of relatively thick MnIr/CoFe(pinned) on top of underlayer/bufferlayer, we presume that the actual h values would likely be higher than the rms

roughness values taken on top of bufferlayers in three sample sets. Having considered above, the H_{in} value of 30 Oe observed in the junction (b) is higher compared to the model value of about 10 Oe at most if we plug the roughness of 0.06 nm into the model. More detailed assessment of the actual h and λ would be of interest to better explain the H_{in} behavior, but this is beyond the scope of this study.

The change of MR ratios of various MTJ structures upon exposure to annealing is shown in Fig. 3. Multiple samples were prepared and annealed to confirm reproducibility as indicated by error bars. Note that all measurements were done at RT. The MR ratio of the MTJ without an NOL (sample (a)) decreased significantly above 200 $^{\circ}\text{C}$. The MTJ structure where an NOL was placed inside the underlayer (sample (b)) maintained its MR ratio up to 250 $^{\circ}\text{C}$. Lastly, the structure with an NOL inside the bufferlayer (sample (c)) withstood till 300 $^{\circ}\text{C}$ without an abrupt loss in the MR ratio.

The primary result of this letter is illustrated in Fig. 4. To uncover the cause of thermal degradation of MR ratios observed above, we have performed AES analysis by tracing elemental Mn of three MTJ samples annealed at 300 $^{\circ}\text{C}$ for 1 h. It should be noted that the AES analysis only offers relative interdiffusion information rather than an absolute one because the depth profiling was carried out at the scanning rate of 1 nm/s and elemental mixing was inevitable during sputter etching of layers. Therefore, the dotted lines in Fig. 4 are qualitative and included for eye-guiding purpose only. The MTJ without an NOL (sample (a)) has asymmetric Mn interdiffusion profile where Mn pumped out from IrMn was attracted toward AlO_x tunnel barrier. The oxygen in the barrier provides high chemical potential for Mn diffusion because the electronegativity difference between Mn (1.55) and O (3.44) is large. Meanwhile the NOL placed samples (b) and (c) exhibited a symmetric Mn profile which manifests the fact that Mn was attracted rather evenly toward both sides of oxides: one

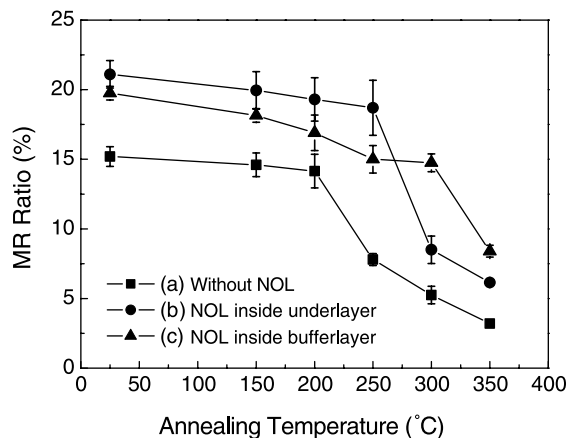


Fig. 3. TMR ratio changes as a function of annealing temperature for three MTJs. All measurements were made at RT. Multiple sets of samples per each structure were prepared and tested.

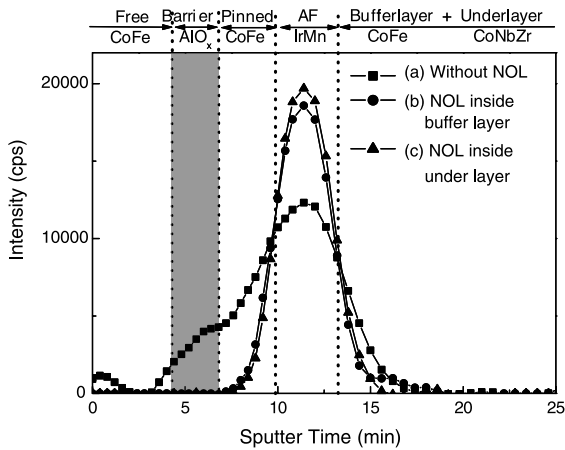


Fig. 4. AES depth profiles of Mn in three MTJ structures after annealing at 300 °C for 1 h. Dotted lines qualitatively indicate estimated interfaces between layers.

toward the barrier (to left), while the other to the NOL (to right). As a consequence, Mn diffusion to the barrier was effectively retarded. The presence of NOL appears to play some role as a mean to control the direction of Mn diffusion. We think this is why we have observed better thermal stability for MTJ samples with NOLs in Fig. 3.

In conclusion, we devised an MTJ structure where an NOL layer was formed inside the underlayer or bufferlayer located under the IrMn. These structures, in general, exhibited improved thermal stability of magnetoresistive properties upon annealing compared to junctions without NOL. It was found that NOL dragged Mn atoms so that Mn diffusion toward the barrier was largely reduced.

Acknowledgements

This work was supported by the National Research Laboratory Program and by the National Program for Tera-level Nanodevices of the Korea Ministry of Science and Technology as one of the 21st century Frontier Programs. Y.K. Kim acknowledges the support of the Dupont Young Professor Fellowship.

References

- [1] S.S.P. Parkin, K.P. Roche, M.G. Samant, P.M. Rice, R.B. Beyers, R.E. Scheuerlein, E.J. O'Sullivan, S.L. Brown, J. Buchigano, D.W. Abraham, Y. Lu, M. Rooks, P.L. Trouilloud, R.A. Wanner, W.J. Gallagher, *J. Appl. Phys.* 85 (1999) 5828.
- [2] S. Cardoso, R. Ferreira, P.P. Freitas, P. Wei, J.C. Soares, *Appl. Phys. Lett.* 76 (2000) 3792.
- [3] Y. Saito, M. Amano, K. Nakajima, S. Takahashi, M. Sagoi, *J. Magn. Magn. Mater.* 223 (2001) 293.
- [4] M.G. Samant, J. Luning, J. Stohr, S.S.P. Parkin, *Appl. Phys. Lett.* 76 (2000) 3097.
- [5] Y. Kamiguchi, H. Yuasa, H. Fukuzawa, K. Kou, H. Iwasaki, M. Sahashi, *International Magnetism Conference, Digest DB-01* 1999.
- [6] H. Fukuzawa, K. Koi, H. Tomita, H.N. Fuke, H. Iwasaki, M. Sahashi, *J. Appl. Phys.* 91 (2002) 6684.
- [7] W.F. Egelhoff Jr., P.J. Chen, C.J. Powell, M.D. Stiles, R.D. McMichael, J.H. Judy, K. Takano, A.E. Berkowitz, *J. Appl. Phys.* 79 (1997) 6142.
- [8] B.S. Chun, S.R. Lee, Y.K. Kim, *J. Appl. Phys.* 93 (2003) 8361.
- [9] J.C. Kools, W. Kula, D. Mauri, T. Lin, *J. Appl. Phys.* 85 (1999) 4466.